U.S. DEPARTMENT OF COMMERCE
NATIONAL OCEANIC AND ATMOSPHERIC ADMINISTRATION
NATIONAL WEATHER SERVICE
NATIONAL METEOROLOGICAL CENTER

OFFICE NOTE 217

Theory of Optimum Interpolation

Ronald D. McPherson
Development Division

JULY 1980

I. Introduction

Statistical interpolation procedures to provide initial conditions for operational numerical weather prediction models were first introduced in the Soviet Union and later in Canada (Kruger, 1969; Rutherford, 1972). This methodology was not seriously considered at NMC until the transition of the data base to a fundamentally nonhomogeneous nature became an established trend. Somewhat earlier, other modeling groups in the international community evinced interest in statistical, or "optimum," interpolation, largely stimulated by activities connected with the Global Atmospheric Research Program. By the middle 1970's, interest in optimum interpolation was widespread. Global assimilation systems based on this concept were being developed at a number of institutions, including the National Center for Atmospheric Research (Schlatter, 1975), the Geophysical Fluid Dynamics Laboratory (Miyakoda et al., 1978), and the National Meteorological Center (Bergman, 1979; McPherson et al., 1979) in the United States, as well as the European Centre for Medium Range Weather Forecasts (Lorenc et al., 1977).

An understanding of the theory of optimum interpolation is necessary to appreciate the reasons for such widespread and continuing interest. This paper represents a general discussion of the theory and illustrates some of its important aspects with simple examples. For a more comprehensive treatment of the theory, the reader would do well to consult the original work of Gandin (1963).[1]

II. Analysis Equations

Consider a scalar field, representing an arbitrary meteorological variable, with a true value at any point in three-dimensional space given by $F(x,y,p)$. We assume that the field is sampled by randomly-distributed imperfect observations $F^o(x_i,y_i,p_i)$ which contain both the truth $F(x_i,y_i,p_i)$ and an error $\varepsilon(x_i,y_i,p_i)$. Thus,

$$F^o(x_i,y_i,p_i) = F(x_i,y_i,p_i) + \varepsilon(x_i,y_i,p_i). \tag{1}$$

The observational error ε may arise from several sources, including instrument error, sampling error, and communications error. We also assume that an estimate of F is available, denoted by $F(x,y,p)$; this field is often called the background field, or "first guess," and by implication is in error to some degree. To correct the error in the background field at a given point, we first estimate the error at the observation locations:

$$f_i^{\,o} = F^o(x_i,y_i,p_i) - \hat{F}(x_i,y_i,p_i) \tag{2}$$

---

[1]The presentation in this paper is largely taken from the paper by Bergman (1979) and unpublished notes prepared by Dr. J. P. Gerrity of NMC.

or, from (1)

$$f_i^o = F(x_i,y_i,p_i) + \varepsilon(x_i,y_i,p_i) - \hat{F}(x_i,y_i,p_i), \tag{3}$$

and then form a linear combination of the f_i^o to provide a corrected estimate, or "analysis," of the true field at a point (ξ,η,ζ):

$$F^a(\xi,\eta,\zeta) = \hat{F}(\xi,\eta,\zeta) + \sum_{i=1}^{n} w_i f_i^o$$

$$= \hat{F}(\xi,\eta,\zeta) + \sum_{i=1}^{n} w_i\{F(x_i,y_i,p_i) + \varepsilon(x_i,y_i,p_i) - \hat{F}(x_i,y_i,p_i)\} \tag{4}$$

Statistical interpolation requires that the coefficients w_i be chosen so as to minimize the mean-square error in the estimate F^a. Thus, introducing the true field on both sides of (14), we obtain

$$F(\xi,\eta,\zeta) - F^a(\xi,\eta,\zeta) \equiv E(\xi,\eta,\zeta)$$

$$= f(\xi,\eta,\zeta) - \sum_{i=1}^{n} w_i[f(x_i,y_i,p_i) + \varepsilon(x_i,y_i,p_i)] \tag{5}$$

where $f = F - \hat{F}$ represents the true error in the background field. The coefficients are determined by requiring that the expected value of E^2 be a minimum. We require

$$\frac{\partial}{\partial w_j}\left(E^2\right) = \frac{\partial}{\partial w_j}\overline{\{f(\xi,\eta,\zeta) - \sum_{i=1}^{n} w_i[f(x_i,y_i,p_i) + \varepsilon(x_i,y_i,p_i)]\}^2} = 0. \tag{6}$$

The notation may be condensed by defining

$$f_i = f(x_i,y_i,p_i)$$

$$f_g = f(\xi,\eta,\zeta).$$

The minimization process indicated in eqn. (6) then results in a system of N equations in the N unknown weights w_j,

$$\sum_{j}^{N} w_j[\overline{f_i f_j} + \overline{\varepsilon_i \varepsilon_j} + \overline{f_i \varepsilon_j} + \overline{f_j \varepsilon_i}] = \overline{f_g f_i} + \overline{f_g \varepsilon_i}, \quad i = 1,N \tag{7}$$

where $\overline{f_i f_j}$ = covariance of the true error $(F - \hat{F})$ in the background field at point (x_i, y_i, p_i) with the true error at point (x_j, y_j, p_j);

$\overline{\varepsilon_i \varepsilon_j}$ = covariance of the observational error at point (x_i, y_i, p_i) with that at point (x_j, y_j, p_j);

$\overline{f_g \varepsilon_i}$, $\overline{f_i \varepsilon_j}$, $\overline{f_j \varepsilon_i}$ = covariance of the true forecast error at one point with the observational error at another point;

$\overline{f_g f_i}$ = covariance at the true forecast error at the point to be updated with the true forecast error at observation point (x_i, y_i, p_i).

It is important to note two implicit assumptions arising from eqn. (7)

- the mean value of $f = F - \hat{F}$ is assumed to vanish;

- the covariances are statistically homogeneous.

It is also important to note that these assumptions are required only locally, in the vicinity of the point being updated, rather than globally.

The assumption of local homogeneity means, for example, that the variance of forecast error

$$\sigma_f^2 = \overline{f_i f_i}$$

is independent of position in the neighborhood of the grid point to be updated. It may, however, vary from neighborhood to neighborhood. This assumption is probably valid most of the time.

Assuming that the long term mean value of the true forecast error at a grid point vanishes is somewhat less valid. For example, it is known that most forecast models underestimate the wind speed in high-wind-speed regions such as jet streams. Thus, the mean value of the forecast error in the eastward wind component of the upper troposphere at a grid point in middle latitudes probably is not zero. The statistical basis for this method is therefore eroded to some degree in such situations, and the interpolated value F^a will in general depart from optimality in the sense implied by eqn. (6).

It is generally assumed that terms (in eqn. 7) of the form $\overline{f_i \varepsilon_j}$ vanish; that is, that errors of observation are not correlated with errors of forecasts. Certain instances can arise where this assumption is questionable but in the present NMC data assimilation system, such terms are not considered.

With these assumptions, eqn. (7) reduces to

$$\sum_{j}^{N} w_j[\overline{f_i f_j} + \overline{\varepsilon_i \varepsilon_j}] = \overline{f_g f_i}, \tag{8}$$

or, in matrix form

$$\begin{pmatrix} (\sigma_f^2 + \overline{\varepsilon_1^2}) & (\overline{f_1 f_2} + \overline{\varepsilon_1 \varepsilon_2}) & (\overline{f_1 f_3} + \overline{\varepsilon_1 \varepsilon_3}) \cdots & (\overline{f_1 f_n} + \overline{\varepsilon_1 \varepsilon_n}) \\ (\overline{f_2 f_1} + \overline{\varepsilon_2 \varepsilon_1}) & (\sigma_f^2 + \overline{\varepsilon_2^2}) & (\overline{f_2 f_3} + \overline{\varepsilon_2 \varepsilon_3}) \cdots & (\overline{f_2 f_n} + \overline{\varepsilon_2 \varepsilon_n}) \\ \vdots & \vdots & \vdots & \vdots \\ (\overline{f_n f_1} + \overline{\varepsilon_n \varepsilon_1}) & + \cdots \cdots \cdots & \cdots & (\sigma_f^2 + \overline{\varepsilon_n^2}) \end{pmatrix} \begin{pmatrix} w_1 \\ w_2 \\ \vdots \\ w_n \end{pmatrix} = \begin{pmatrix} \overline{f_g f_1} \\ \overline{f_g f_2} \\ \vdots \\ \overline{f_g f_n} \end{pmatrix} \tag{9}$$

The coefficient matrix is symmetric and is usually positive definite. If its elements are known, or can be specified, then the system may be solved for the vector of unknown coefficients w_j, given that the right-hand-side is also known or determinable. Once the w_j have been calculated, the analyzed value of F at point (ξ,η,ζ) may be determined from eqn. (4).

Equations (8) or (9) illustrate the mechanism by which the statistical interpolation method treats a nonhomogeneous data base. For the first observation, represented by the top row of eqn. (9), we note that the main diagonal term is composed of the sum of the forecast error variance and the observational error variance $\overline{\varepsilon_1^2}$. We may assign a value to $\overline{\varepsilon_1^2}$ appropriate to the type of observation. Likewise, $\overline{\varepsilon_1^2}$ maybe assigned a different value. In practice, observational errors are assigned by classes: e.g., radiosonde temperatures are assigned an error variance determined for radiosondes, but remote soundings have their own error variance. Examples of values currently used are given in the third lecture of this series, and the determination of these values is discussed in the fourth lecture.

The off-diagonal elements of eqn. (9) also contain error terms of the form $\overline{\varepsilon_i \varepsilon_j}$, $i \neq j$. Such terms describe the tendency of some observational systems to produce reports with spatially correlated errors. For example, errors in remote temperature soundings frequently tend to be of the same sign in local areas--a local "bias." Thus, if a remote sounding at one point can be determined as being too warm, its immediately adjacent neighbor is also likely to be too warm. In such a situation, the covariance between the errors in the two soundings would be nonzero and positive. In contrast, given two nearby radiosonde reports, one of which is apparently too warm, the other is as likely to be too cold as too warm. Consequently, the covariance between the radiosonde errors would vanish.

Before proceeding to a discussion of the determination of the elements of the coefficient matrix and the right-hand vector of eqn. (9), we note for future reference that we may extract from eqn. (6) an expression for the expected error of interpolation, also referred to as the "estimated analysis error";

$$E = f_g - \sum_{i=1}^{N} w_i f_i^o \quad . \tag{10}$$

Thus, once the w_i have been determined, the estimated analysis error may be calculated.

III. Covariance Modeling

Autocovariance

In principle, the several covariances appearing in eqn. (9) can be determined from actual differences between forecasts and observations, and therefore can be updated continuously. Serious difficulties attend this in practice, not the least of which is the necessity of removing the influence of observational error. In part for this reason, and in part for reasons to be addressed in the next section, the covariances are modeled by an analytic function.

Much discussion appears in the literature (see e.g., Thiebaux, 1975) concerning the nature of modeled covariance functions and the sensitivity of the resulting analysis to changes in the functions. General agreement has not yet been firmly established. In the NMC system, it is assumed that the geopotential height autocovariance is of the form

$$(\overline{h_i h_j}) = \sigma^2_h \; e^{-K_h S^2} \; [1 + K_p q^2]^{-1} \tag{11}$$

where h_i is the true forecast error in the geopotential height at point (x_i, y_i, p_i), and h_j is the same quantity at another point (x_j, y_j, p_j). The height forecast error variance is denoted by σ_h^2, $S^2 = (x_i - x_j)^2 + (y_i - y_j)^2$, and $q^2 = [\ell n(p_i) - \ell n(p_j)]$. Equation (11) assumes that the true three-dimensional forecast error covariance can be approximated by the product of a horizontal and a vertical covariance function. The constants K_h and K_p govern the shape of the analytic functions.

Figure 1 illustrates the assumed horizontal component of the analytic autocovariance function for several values of the constant K_h. The covariances have been normalized, and so the curves represent correlations. For $K_h = 0.5 \times 10^{-6}$ K_m^{-2}, the correlation declines quite slowly with increasing separation; it is still nearly 0.5 at 1200 km. For largest value plotted, the correlation reduces to less than 0.5 beyond about 700 km. The actual value currently used, 0.98×10^{-6} km^{-2}, is approximately illustrated by the dashed curve in the diagram.

Figure 1. Horizontal component of the $\overline{hh}$ covariance for several values of the constant K_h. The dashed curve is approximately that used in the NMC Global Data Assimilation System. Curves have been normalized by the forecast error variance.

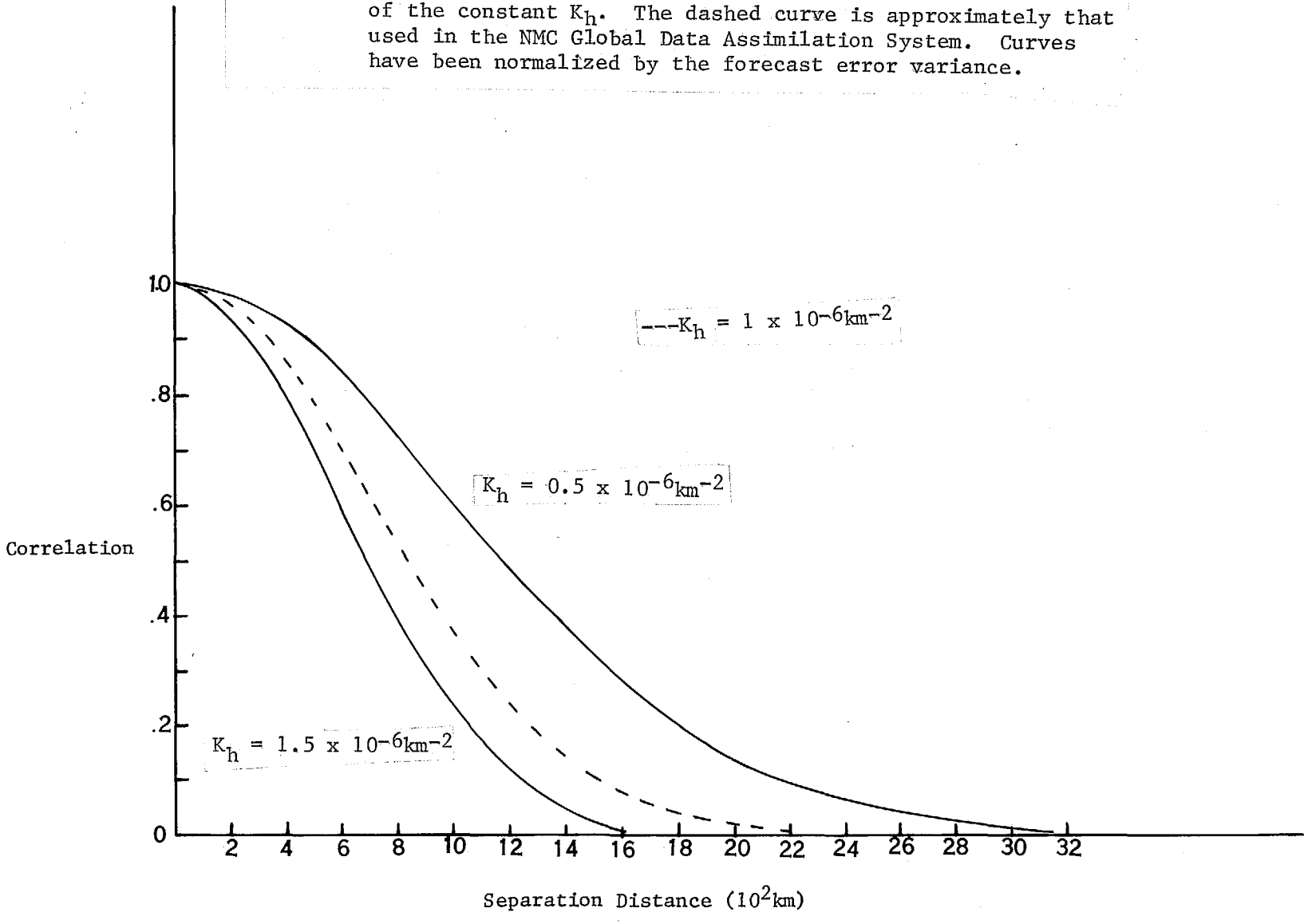

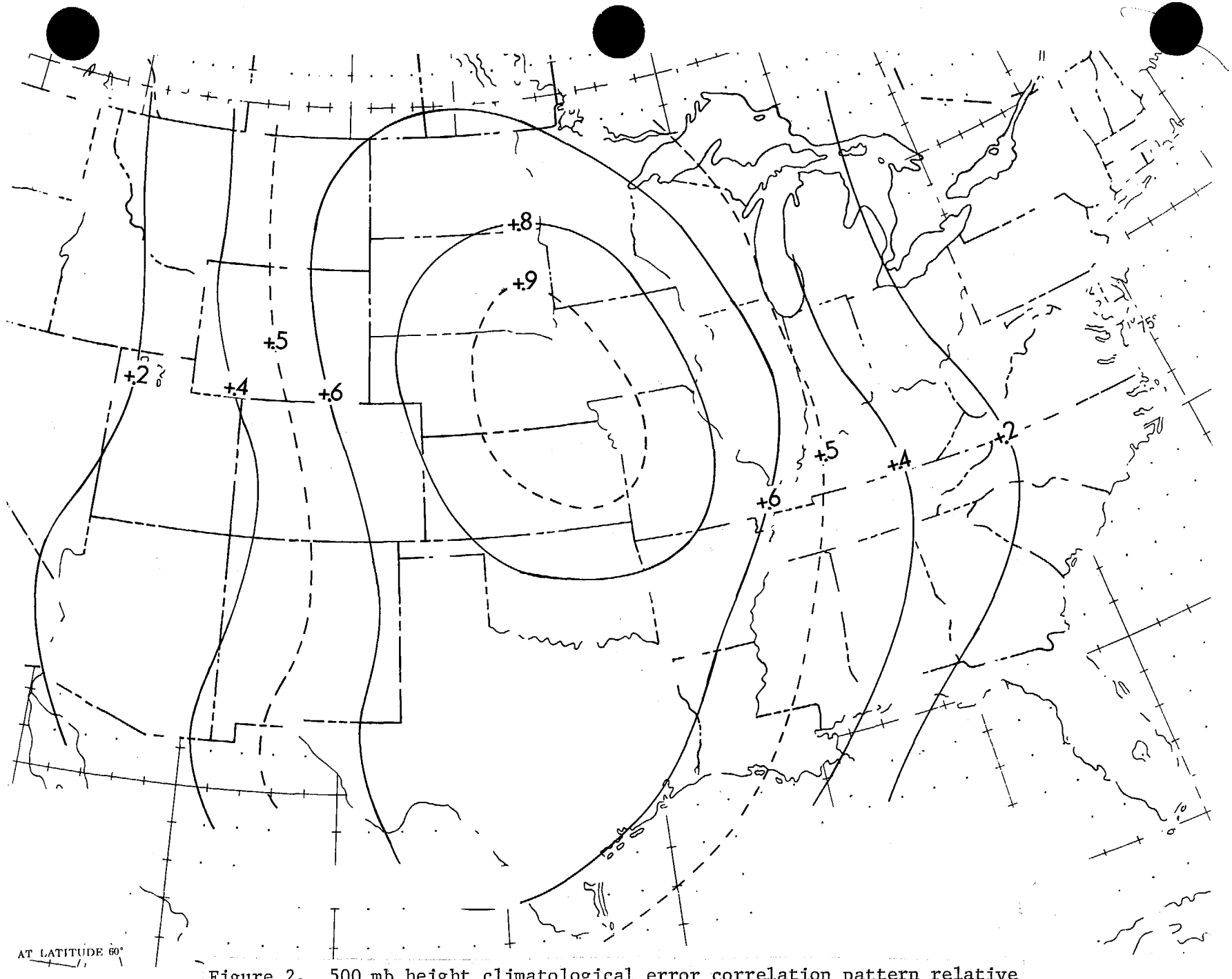

Figure 2. 500 mb height climatological error correlation pattern relative to Omaha, Nebraska, for December 1978 - February 1979.

Figures 2 and 3 show actual correlations for climatological and forecast errors respectively. These were calculated by forming residuals between the background field and radiosonde observations for a network of stations over North America. Covariances were then calculated with respect to the residual at Omaha, Nebraska, and normalized. The resulting correlations are illustrated in the two diagrams, for December 1978 through February 1979.

Figure 2 depicts the result when the background field is climatology. The pattern is distinctly elliptical, with its major axis oriented meridionally. This is somewhat unusual--most such patterns are more circular--and may be due to particularly persistent weather patterns in that particular winter. An estimate of the average distance from Omaha to the 0.5 contour turns out to be about 1200 km, in approximate agreement with the curve in Fig. 1 for $K_h = 0.5 \times 10^{-6}$ km^{-2}. Thus, this value may be thought of as appropriate when the residuals are computed from a climatological background field.

When the residuals are calculated using a short-range forecast of the NMC nine-layer global prediction model as the background, a more nearly isotropic pattern with smaller magnitudes results. This is illustrated in Fig. 3, also for December 1978 through February 1979. The area inside the 0.5 isoline is much reduced by comparison to Fig. 2, and the average distance from Omaha to that contour is about 700 km. This compares favorably with the $K_h = 1.5 \times 10^{-6}$ km^{-2} curve in Fig. 1. The value in actual use, 0.98×10^{-6} km^{-2}, is treated as a universal value. It thus represents a compromise between a value of K_h based on forecast errors in an area where forecasts are of relatively high quality, and one which assumes a deterioration of forecast quality toward climatological skill over data-sparse areas.

The vertical component of the height autocovariance function is illustrated in Figs. 4 and 5. In the former, $p_i = 700$ mb, and the autocovariances are therefore calculated with respect to 700 mb. In the latter, $p_i = 250$ mb. Normalized (correlation) curves for two values of K_p are displayed. The circles indicate actual vertical correlations of forecast error at Omaha for the December 1978-February 1979 data set. For $K_p = 5$, the correlation decreases more rapidly away from p_i than with $K_p = 1.5$. Actual correlations at Omaha lie between the two values for $p_i = 250$ mb. For the lower level, the agreement below 700 mb between the data and $K_p = 5$ is excellent. However, the agreement is not as good at higher levels. Nevertheless, $K_p = 5$ is the value presently used in the NMC system.

Scale Considerations

The covariance function defined by eqn. (11) is applied to a field of residuals which contains a spectrum of scales of atmospheric phenomena. If the individual residuals were completely independent, this function could be thought of as a filter, the response of which is given by its Fourier transform. Figure 6a gives the normalized covariance as a function of separation for $K_h = .98 \times 10^{-6}$ km^{-2}, while the lower part of the diagram presents the Fourier transform of the upper curve.

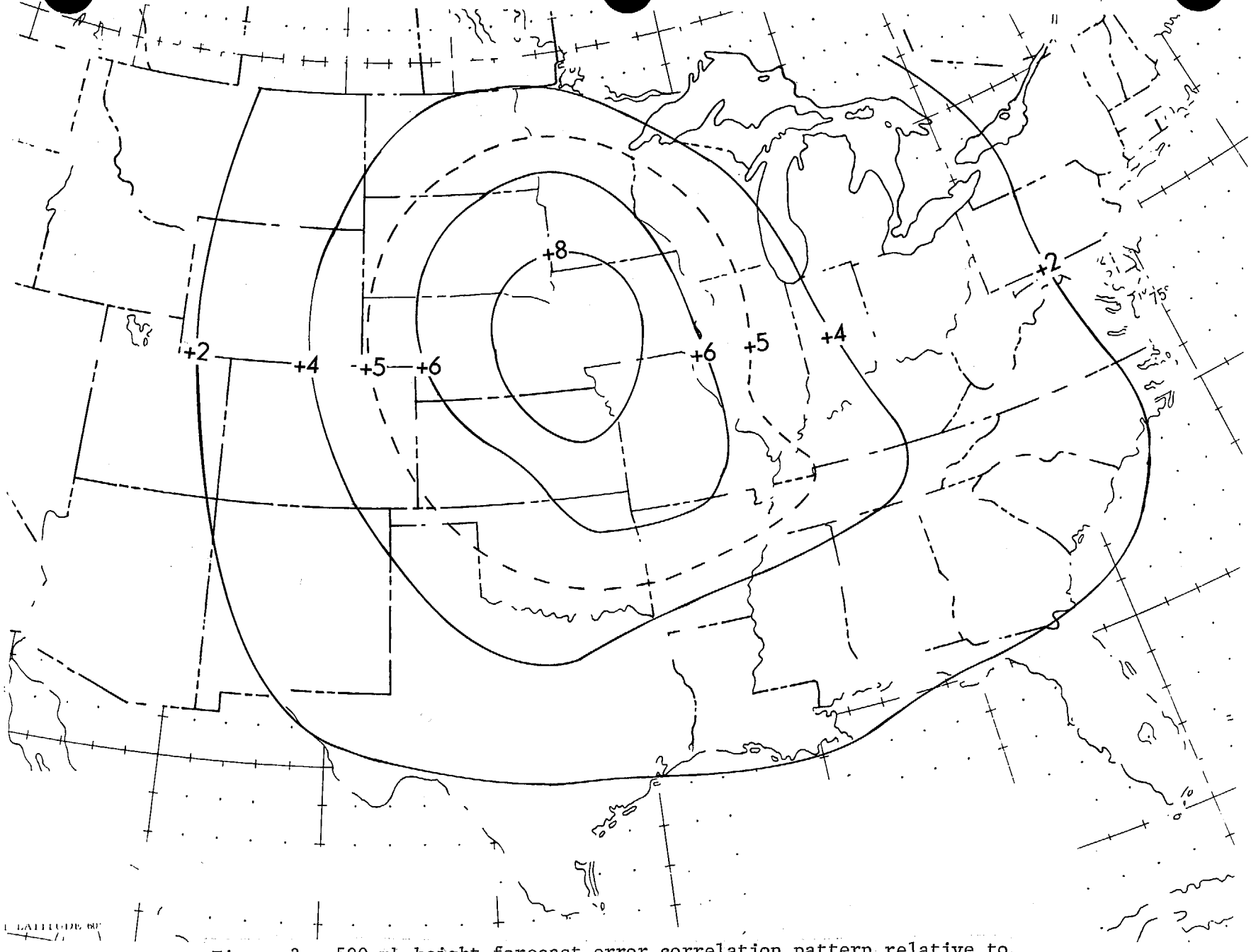

Figure 3. 500 mb height forecast error correlation pattern relative to Omaha, Nebraska, for December 1978 - February 1979.

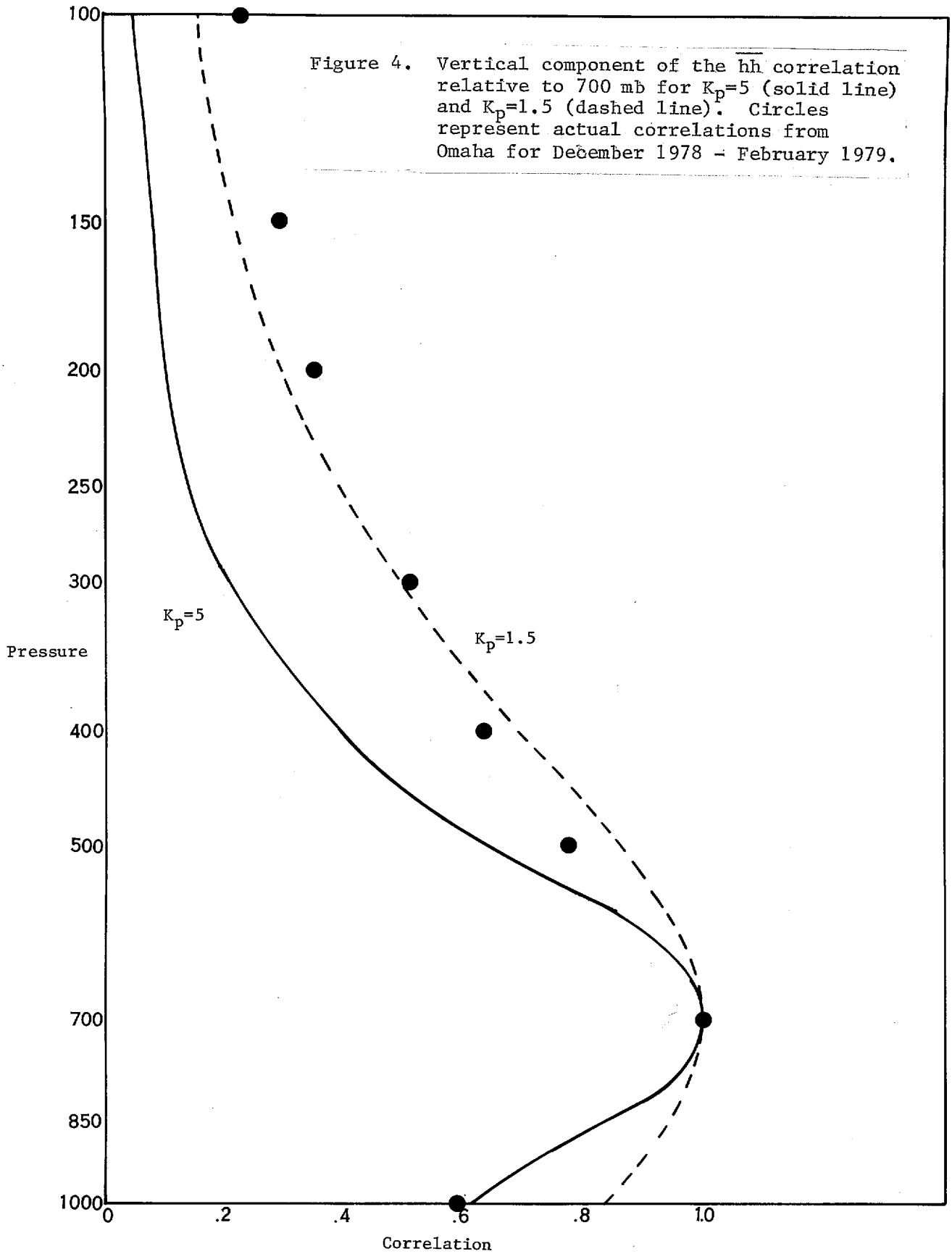

Figure 4. Vertical component of the $\overline{hh}$ correlation relative to 700 mb for K_p=5 (solid line) and K_p=1.5 (dashed line). Circles represent actual correlations from Omaha for December 1978 - February 1979.

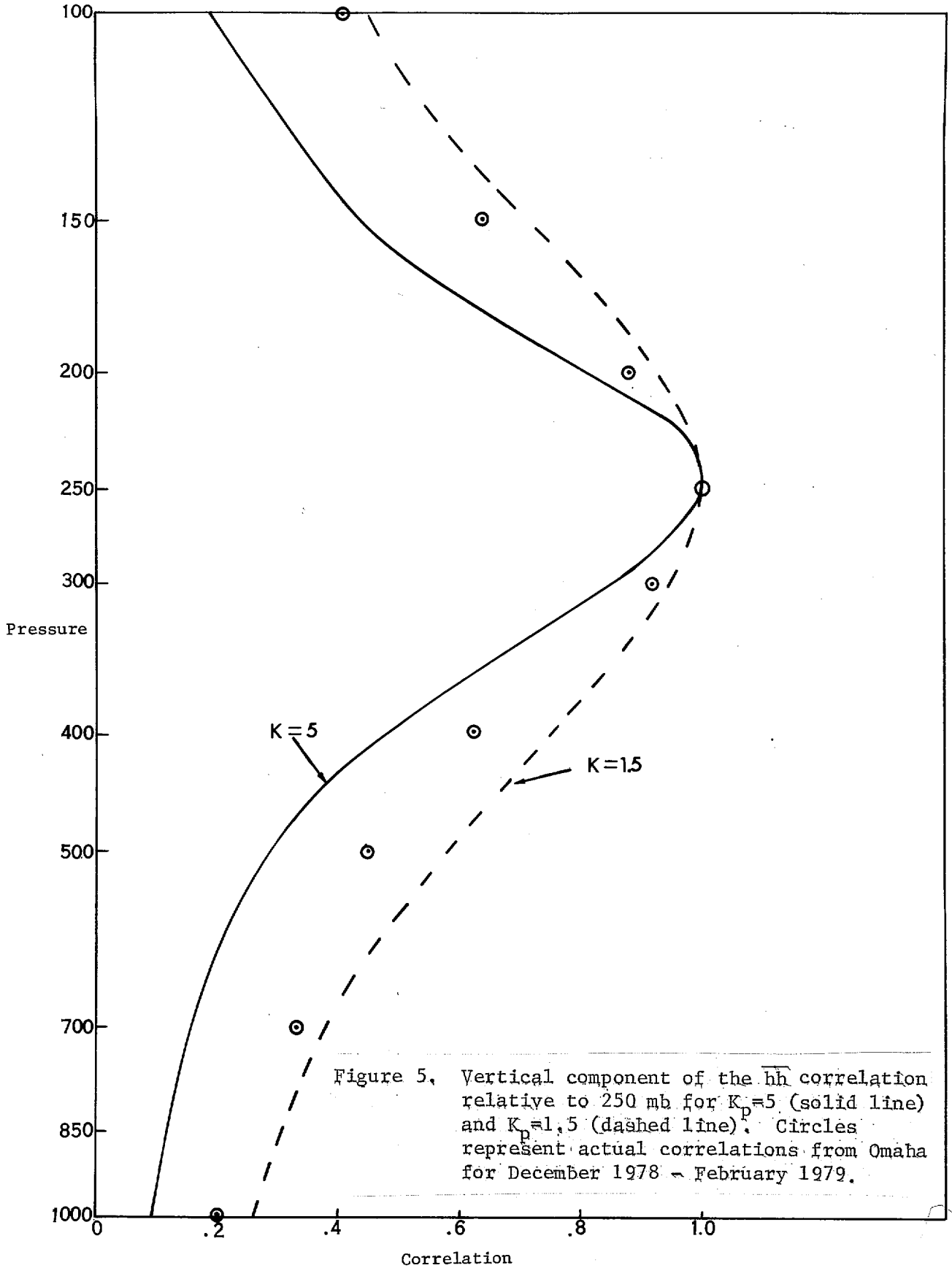

Figure 5. Vertical component of the $\overline{hh}$ correlation relative to 250 mb for K_p=5 (solid line) and K_p=1.5 (dashed line). Circles represent actual correlations from Omaha for December 1978 - February 1979.

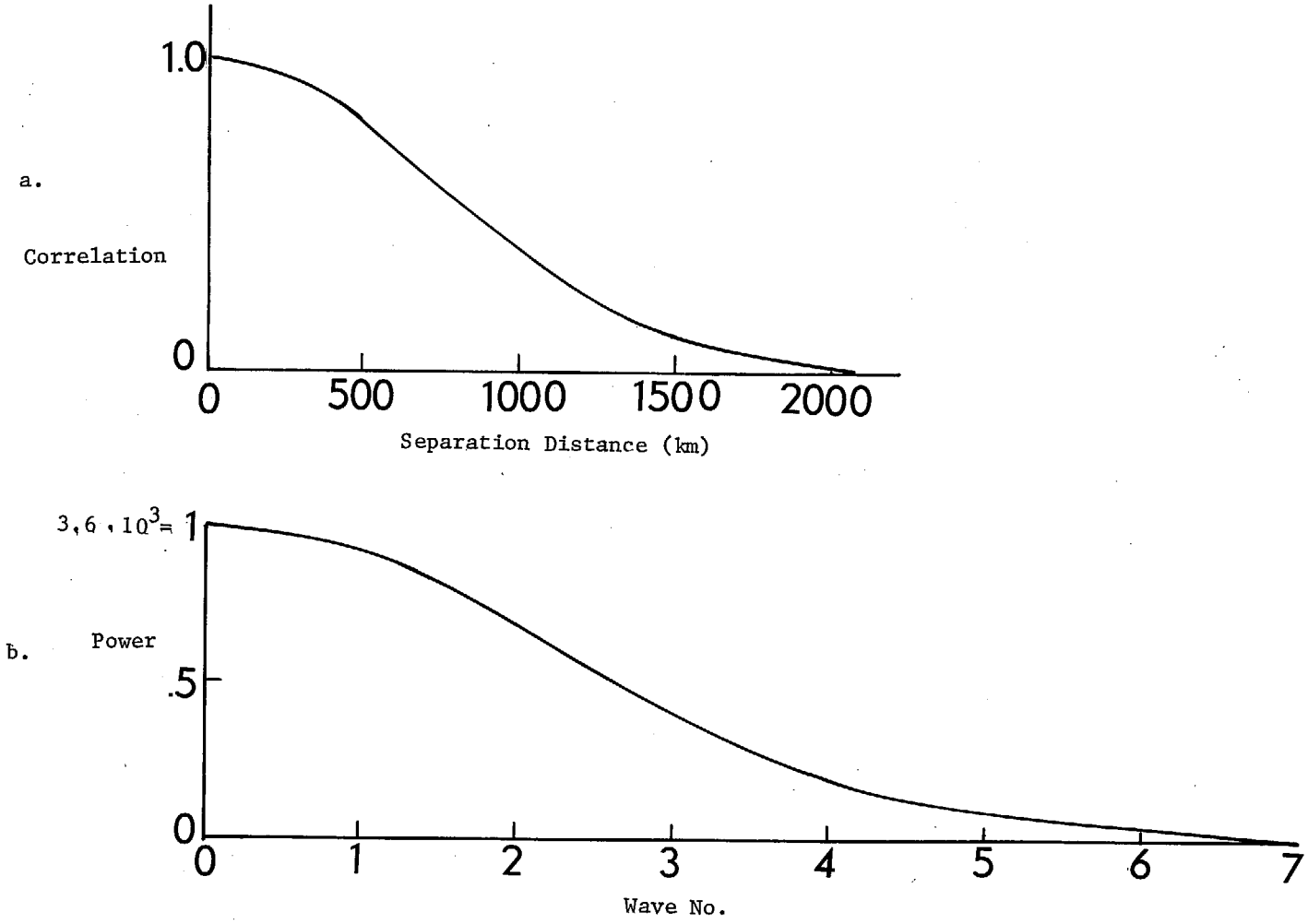

Figure 6. (a) $\overline{hh}$ correlation as a function of separation distance for $K_H = .98 \times 10^{-6} km^{-2}$.
(b) Fourier transform of the $\overline{hh}$ correlation. Power density as a function of wave number $fx10^{-4} km^{-1}$.

For this extreme example, Figure 6b shows that small-scale patterns in the residual field--wavelengths less than about 5000 km--could not be accurately represented. Patterns with wavelengths of 3000 km would have their amplitudes underestimated by 60%. Only those patterns with wavelength longer than 10,000 km would be represented in the analysis with reasonable fidelity. This would obviously represent a severe limitation on the scales of phenomena that can be represented.

However, the assumption of independence is not valid. The statistical interpolation method explicitly considers interobservational correlation. Consequently, the covariance function cannot be thought of as a filter. The actual weighting function is much more complicated; in particular it is dependent on data distribution. A general response function is not easily defined.

Cross-covariance

If one wishes to permit observations of the mass field to influence the analysis of the motion field, and vice versa, this can be accomplished by assuming that the residuals of the mass and motion fields behave in accordance with the geostrophic and hydrostatic relationships. This is the second reason for the assumption of analytic, differentiable forms for the $\overline{hh}$ covariance.

Consider as an example the covariance of east wind component $u(\xi,\eta,\zeta)$ with the geopotential height at some other point (x,y,z), where $(\zeta,z) = \ell n(\text{pressure})$. The geostrophic equation may be written as

$$u(\xi,\eta,\zeta) = -\frac{g}{f}\frac{\partial}{\partial y} h(\xi,\eta,\zeta) \quad . \tag{12}$$

Let us form the covariance function $\overline{u(\xi,\eta,\zeta)\, h(x,y,z)}$ by multiplying both sides of eqn. (12) by $h(x,y,z)$ and averaging over many pairs of u and h. Thus

$$\overline{u(\xi,\eta,\zeta)\, h(x,y,z)} = -\frac{g}{h}\overline{\left(\frac{\partial}{\partial \eta} h(\xi,\eta,\zeta)\right)\cdot h(x,y,z)} \tag{13}$$

Introducing the definition of the partial derivative,

$$\overline{u(\xi,\eta,\zeta)\, h(x,y,z)}$$

$$= \frac{g}{f}\lim_{\Delta\eta\to 0}\overline{\frac{h(\xi,\eta+\Delta\eta,\zeta) - h(\xi,\eta,\zeta)}{\Delta\eta}\cdot h(x,y,z)} \tag{14}$$

or

$$= -\frac{g}{f}\lim_{\Delta\eta\to 0}\overline{\frac{h(\xi,\eta+\Delta\eta,\zeta)\cdot h(x,y,z) - h(\xi,\eta,\zeta)h(x,y,z)}{\Delta\zeta}} \quad . \tag{15}$$

But the bracketed quantity is the definition of the partial derivative of the product, so that

$$\overline{u(\xi,\eta,\zeta)\ h(x,y,z)} = -\frac{g}{f}\frac{\partial}{\partial\eta}\overline{[h(\xi,\eta,\zeta)\ h(x,y,z)]}\ . \tag{16}$$

It may also be shown that

$$\overline{h(x,y,z)\ u(\xi,\eta,\zeta)} = -\frac{g}{f}\frac{\partial}{\partial y}\overline{[h(x,y,z)\ h(\xi,\eta,\zeta)]}\ . \tag{17}$$

Similarly, one can derive the $\overline{uu}$ autocovariance. First, multiply eqn. (12) by u(x,y,z) and average over many pairs:

$$\overline{u(\xi,\eta,\zeta)\ u(x,y,z)} = -\frac{g}{f}\frac{\partial}{\partial y}[\overline{h(\xi,\eta,\zeta)\ u(x,y,z)}]\ . \tag{18}$$

Using the definition of the partial derivative

$$= -\frac{g}{f}\overline{\lim_{\Delta\eta\to 0}\frac{h(\xi,\eta+\Delta\eta,\zeta)-h(\xi,\eta,\zeta)}{\Delta\eta}\cdot u(x,y,z)} \tag{19}$$

or

$$= -\frac{g}{f}\lim_{\Delta\eta\to 0}\overline{\frac{h(\xi,\eta+\Delta\eta,\zeta)\ u(x,y,z)-h(\xi,\eta,\zeta)\ u(x,y,z)}{\Delta\eta}} \tag{20}$$

or

$$\overline{u(\xi,\eta,\zeta)\ u(x,y,z)} = -\frac{g}{f}\frac{\partial}{\partial\eta}\overline{h(\xi,\eta,\zeta)\ u(x,y,z)}\ . \tag{21}$$

But from eqn. (17), $\overline{h(\xi,\eta,\zeta)\ u(x,\ y,\ p)}$ may be replaced to obtain

$$\overline{u(\xi,\eta,\zeta)\ u(x,y,z)} = \frac{g}{f^2}\frac{\partial^2}{\partial\eta\partial y}\overline{[h(\xi,\eta,\zeta)\ h(x,y,z)]}. \tag{22}$$

We now consider cross-covariances between geopotential height and temperature: the hydrostatic equation may be written as

$$t(\xi,\eta,\zeta) = -\frac{g}{R}\frac{\partial}{\partial\zeta}h[\xi,\eta,\zeta]\ . \tag{23}$$

Multiplying both sides by h(x,y,z) and averaging over many pairs, we obtain the cross-covariance $\overline{h(x,y,z)\ t(\xi,\eta,\zeta)}$:

$$\overline{h(x,y,z)\ t(\xi,\eta,\zeta)} = -\overline{\frac{g}{R}h(x,y,z)\lim_{\Delta\zeta\to 0}\frac{h(\xi,\eta,\zeta+\Delta\zeta)-h(\xi,\eta,\zeta)}{\Delta\zeta}} \tag{24}$$

or

$$= -\frac{g}{f}\lim_{\Delta\zeta\to 0}\frac{\overline{h(x,y,z)\ h(\xi,\eta,\zeta+\Delta\zeta)} - \overline{h(x,y,z)\ h(\xi,\eta,\zeta)}}{\Delta\zeta} \tag{25}$$

or

$$\overline{h(x,y,z)\ t(\xi,\eta,\zeta)} = -\frac{g}{f}\frac{\partial}{\partial\zeta}\overline{h(x,y,z)\ h(\xi,\eta,\zeta)} \tag{26}$$

In a manner completely analogous to the determination of $\overline{uu}$, the temperature autocovariance can also be obtained:

$$\overline{t(x,y,z)\ t(\xi,\eta,\zeta)} = \left(\frac{g}{R}\right)^2\frac{\partial^2}{\partial z\partial\zeta}\overline{[h(x,y,z)\ h(\xi,\eta,\zeta)]} \tag{27}$$

Indeed, all of the cross-covariances and autocovariances necessary to perform a complete analysis of h, t, u, and v can be derived from the height autocovariance $\overline{hh}$ under the assumptions of geostrophic and hydrostatic balance among the residuals. Table 1 gives the complete set.

Table 1. Covariance of the row variable with the column variable in terms of the geopotential autocovariance $\overline{hh}$, assuming that height, temperature, and wind residuals are related through the geostrophic and hydrostatic equations.

	h	t	u	v
h	$\overline{hh}$	$-\frac{g}{R}\frac{\partial\overline{hh}}{\partial z}$	$-\frac{g}{f}\frac{\partial\overline{hh}}{\partial y}$	$\frac{g}{f}\frac{\partial\overline{hh}}{\partial x}$
t	$-\frac{g}{R}\frac{\partial\overline{hh}}{\partial\zeta}$	$\left(\frac{g}{R}\right)^2\frac{\partial^2\overline{hh}}{\partial\zeta\,\partial z}$	$\frac{g^2}{fR}\frac{\partial^2\overline{hh}}{\partial\zeta\,\partial y}$	$-\frac{g^2}{fR}\frac{\partial^2\overline{hh}}{\partial\zeta\,\partial x}$
u	$-\frac{g}{f}\frac{\partial\overline{hh}}{\partial\eta}$	$\frac{g^2}{fR}\frac{\partial^2\overline{hh}}{\partial\eta\partial z}$	$\frac{g^2}{f^2}\frac{\partial^2\overline{hh}}{\partial\eta\partial y}$	$-\frac{g^2}{f^2}\frac{\partial^2\overline{hh}}{\partial\eta\partial x}$
v	$\frac{g}{f}\frac{\partial\overline{hh}}{\partial\xi}$	$-\frac{g^2}{fR}\frac{\partial^2\overline{hh}}{\partial\xi\partial z}$	$-\frac{g^2}{f^2}\frac{\partial^2\overline{hh}}{\partial\xi\partial y}$	$\frac{g^2}{f^2}\frac{\partial^2\overline{hh}}{\partial\xi\partial x}$

Figure 7 displays the horizontal elements of Table 1 in terms of the correlation defined as the covariance normalized by the variance. A value of $K_h = 0.98 \times 10^{-6}$ km^{-2} has been used. Those elements which involve vertical variations, such as $\overline{ut}$, are shown in Fig. 9. Several points are worth noting from Fig. 7, especially with regard to the derived quantities. Consider, for example, the $\overline{hu}$ correlation. The diagram should be interpreted as illustrating the correlation of u-residuals in the domain with the height residual to be analyzed at the central point of the diagram.

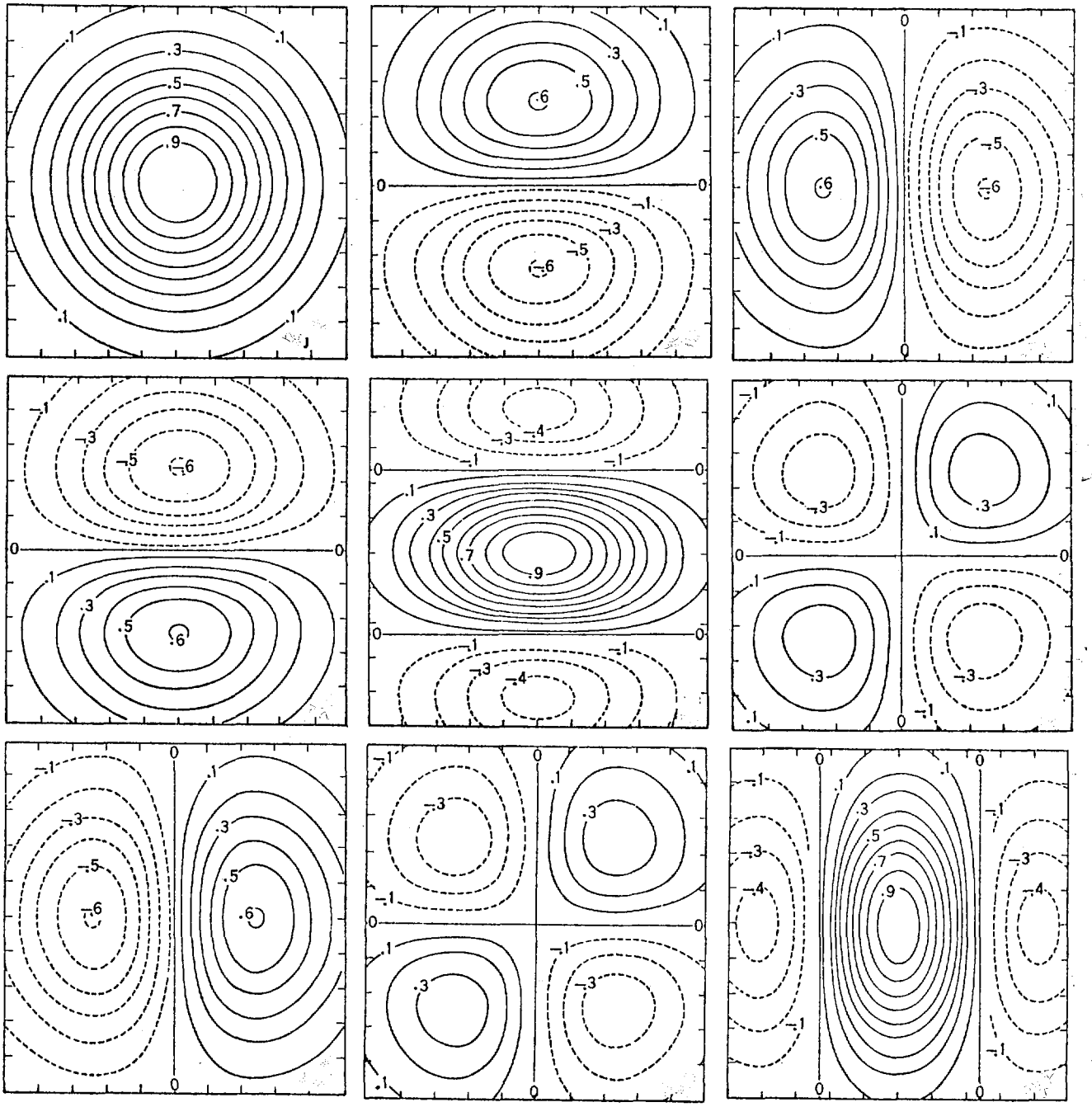

Figure 7. Horizontal correlation functions for geopotential and wind. Left to right, top row: h-h, h-u, h-v; middle row: u-h, u-u, u-v; botton row: v-h, v-u, v-v. Distance intervals correspond to 300 km. After Bergman (1979).

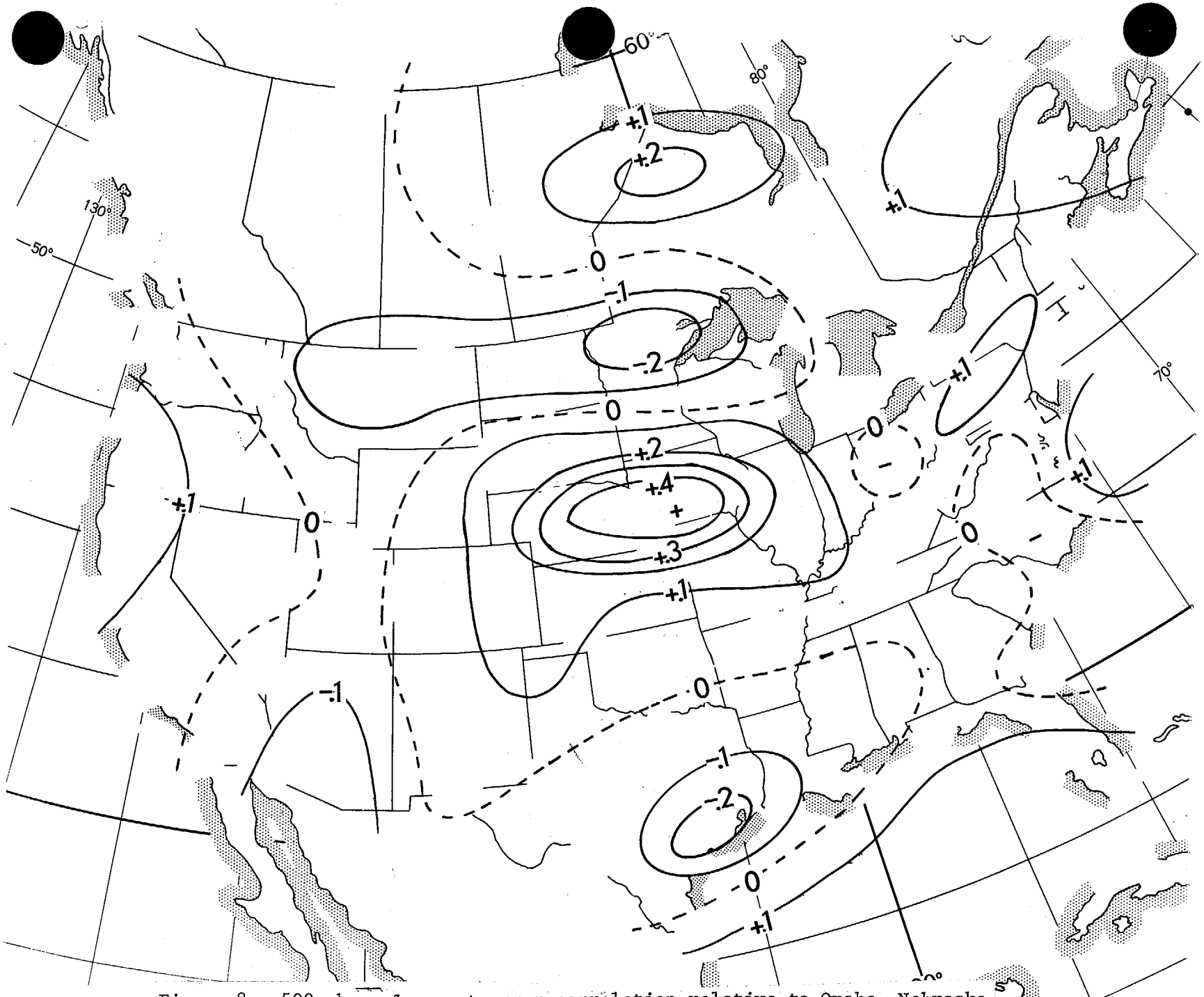

Figure 8. 500 mb $\overline{uu}$ forecast error correlation relative to Omaha, Nebraska, for December 1978 - February 1979.

In this framework, a positive u-residual (forecast u-component is too slow) at the center of the negative lobe south of the grid point implies that the geopotential at the central point should be decreased. Note that an observed u-residual has zero correlation with the height residual along the x-coordinate of the grid point being analyzed. Also, the maximum correlation is slightly greater than 0.6 in absolute value, and occurs approximately 750 km north and south of the grid point. This distance is a function of the assumed correlation function (eqn. 11) and specifically depends on the value of K_h. Thus there is a scale limitation implicit in the forecast error statistics, and one manifestation of this may be noted in that the maximum effect of a wind observation will be realized in the mass analysis 750 km distant from the observation.

Another noteworthy point is that the derived covariances or correlations are not isotropic. Consider the derived $\overline{uu}$, for example: the area of maximum positive correlation is elongated in the upwind-downwind directions. Figure 8, depicting actual $\overline{uu}$ correlations based on the Omaha network for December 1978 through February 1979, confirms the general pattern of this derived function.

One final point to be gleaned from the derived horizontal correlation functions is that the u- and v-components of a given wind observation will have different effects on the u- and v-analysis of a particular grid point. Consider, for example, an observation located on the x-axis of the $\overline{uu}$ field, but about 650 km west of the central point. An observed u-component residual has a correlation of about 0.6 with the analyzed u-correction, but the observed v-component residual has zero correlation with the analyzed v-correction at the same central point.

We now consider the vertical components of the derived covariances. Figure 9 displays the correlation functions corresponding to the vertical parts of $\overline{ht}$ and $\overline{ut}$ as derived from $\overline{hh}$, which is itself reproduced from Fig. 5 for comparison. All curves indicate the correlation of the first variable at 250 mb with the second variable at all pressure levels. The cross-correlation functions plotted in Fig. 9 are derived in the Appendix. As noted previously, there is reasonable agreement between the modeled curve for hh and actual correlations calculated for December 1978-February 1979. The modeled curve does decline away from the level of application more sharply than is indicated by the data, but the shape is in quite good agreement.

The correlation between height and temperature shows a zero when the two are at the same level, and extrema a short distance away. In accordance with expectations based on hydrostatic equilibrium, positive (warm) temperature residuals below the level of the height contribute to an increase in the height there. Likewise, a positive height change results from negative (cold) temperature residuals above the level of the height. It is of interest to note that the level of application is arbitrary; in particular,

Figure 9. Analytic hh (solid line), ht (short dash), and ut (long dash) correlations relative to 250 mb. Boxes denote the actual $\overline{hh}$ correlations for Omaha, December 1978 - February 1979.

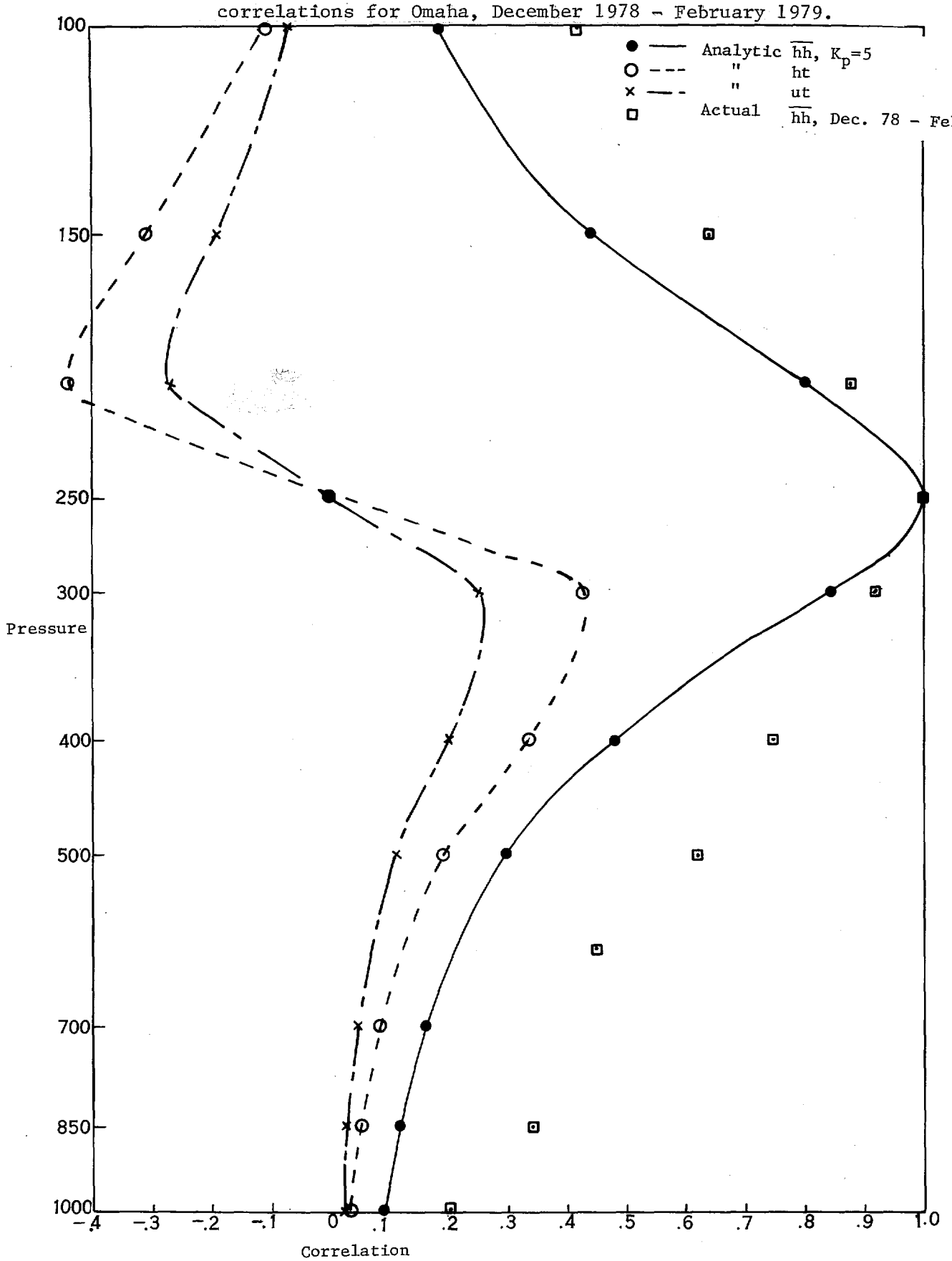

it can be specified as 1000 mb, in which case the correlation curve corresponding to the ht appears as in Fig. 10. A profile of temperature residuals can therefore be used to specify--through the cross-correlations--a height residual at 1000 mbs. Thus it is possible to infer from sounding data alone information on the shape of a level near the surface, which might be used as a reference level. This possibility is considered further in a later section.

We note also from Fig. 9 that the correlation curve corresponding to the ut covariance has relatively small amplitude; that is, the temperature residual at any level does not convey much information about the wind residual at any other level. This is because the temperature gradient relates only to the wind shear, not to the wind itself. A reference level specification is necessary to determine the wind. One way this may be done is to integrate the hydrostatic equation to convert the temperature to height, so that the wind at any pressure is related to the geopotential height gradient at that pressure. When this is done statistically, the correlation pattern appears as in Fig. 7. The correlation pattern corresponding to uh has a maximum greater than 0.6 in absolute value, or roughly double the maximum of the correlation between winds and temperatures.

An example is presented in the next section which further explores the relationships among heights, temperatures, and winds, and offers a suggestion to profitably take advantage of those relationships in the analysis system.

IV. Examples of the Theory and Its Implications

Cross-correlation analysis

Consider a profile of temperature residuals defined by the second column of Table 2. Note that these are differences between predicted and observed layer-mean temperatures, and so are assigned to pressures representing midpoints between standard pressure levels. According to the theory outlined in the previous section, height residuals can be calculated from the temperature residuals. For any level ,

$$h = a\,t + a\,t + \ldots + a\,t \,, \tag{28}$$

where the a_i can be determined by solving the system

$$t_k t_i\, a_i = h\, t_k, \quad k = 1,10 \tag{29}$$

The resulting h for standard pressure levels from 1000 mb to 100 mb are given in the third column of Table 2.

Cross-correlation analysis

Consider a profile of temperature residuals defined by the second column of Table 2. Note that these are differences between predicted and observed layer-mean temperatures, and so are assigned to pressures representing midpoints between standard pressure levels. According to the theory outlined in the previous section, height residuals can be calculated from the temperature residuals. For any level ℓ,

$$h_\ell = a_1 t_1 + a_2 t_2 + \ldots + a_{10} t_{10}, \tag{28}$$

where the a_i can be determined by solving the system

$$t_k t_i \, a_i = h \, t_k, \quad k = 1,10 \tag{29}$$

The resulting h_ℓ for standard pressure levels from 1000 mb to 100 mb are given in the third column of Table 2.

$$h_\ell = a_1 t_{928} + a_2 t_{777} + \ldots + a_{10} t_{85}, \tag{28}$$

where the a_i can be determined by solving the system

$$\sum_{i=1}^{10} t_k t_i \, a_i = h_\ell t_k, \quad k = 1,10 \tag{29}$$

The resulting h_ℓ for standard pressure levels from 1000 mb to 100 mb are given in the third column of Table 2.

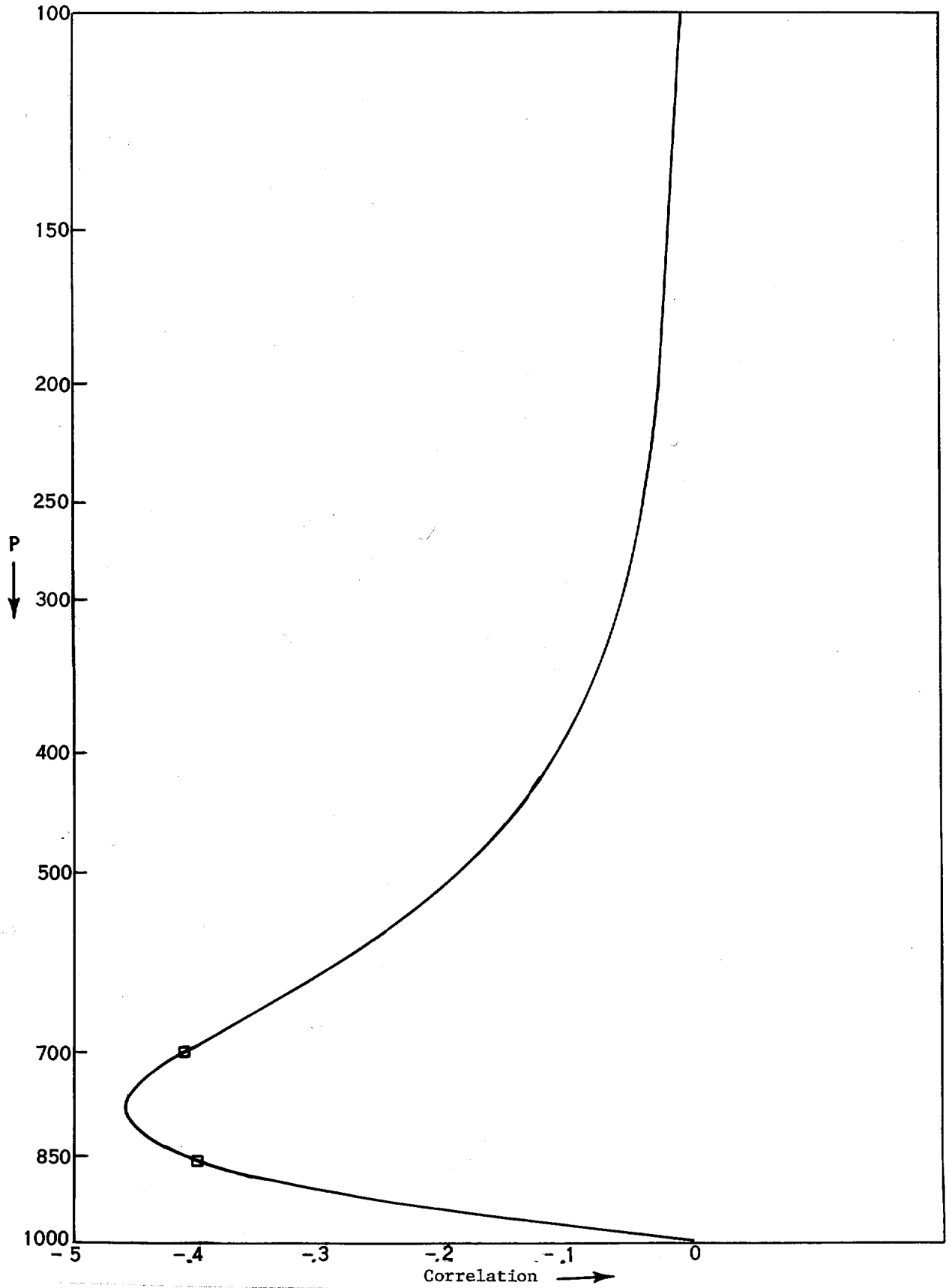

Figure 10. Analytic $\overline{ht}$ correlation between 1000 mb height and temperatures at higher levels.

We next consider the determination of a u-component residual of 400 mb from the height and temperature profiles. First, let

$$u_{400} = a_1 t_{928} + a_2 t_{777} + \ldots + a_{10} t_{85} \tag{30}$$

and calculate the weights a_i by solving the system

$$\sum_{i=1}^{10} \overline{t_k t_i}\, a_i = \overline{u_\ell t_k} \,. \tag{31}$$

These weights are presented in column 4 of Table 2. Note that they are all fairly small, uniformly negative at low levels and uniformly positive in high levels, and tending toward cancellation. Importantly, note that the smallest weight is an appreciable fraction of the largest (in absolute value). Thus temperature information at all levels contributes to the wind analysis at a given level; in this case, the calculated u-component residual at a point assumed to be 750 km away from the temperature residual profile is -0.43 m sec^{-1}.

Next, consider the determination of u_{400} from the height residuals, which were themselves calculated from the temperature residuals:

$$u_{400} = b_1 h_{1000} + b_2 h_{850} + \ldots b_{10} h_{100} \,. \tag{32}$$

The weights b_j may be calculated by solving

$$\sum_{j=1}^{10} \overline{h_k h_j} b_j = \overline{u\, h_k} \,, \qquad k = 1,10 \tag{33}$$

The weights appear in the fifth column of Table 2. Both above and below 400 mb, the weights are small and alternate in sign at adjacent levels. At 400 mb, however, the influence of h_{400} is dominant in determining u; as in the previous instance, $u_{400} = -0.43$ m sec^{-1}. This is further confirmed in column 6, which shows the weight assigned to h_{400} when only that prediction is used in the determination of u_{400}; once again, $u_{400} = -0.43$ m sec^{-1}.

Finally, u_{400} was calculated using only the two temperature residuals immediately adjacent to the 400 mb level. The weights in this case are given in column 7. They are opposite in sign and nearly equal in magnitude, and the value of u_{400} is -0.07 m sec^{-1}.

Thus it appears that the information content of an entire profile of temperature residuals with respect to determining the wind at some level can be condensed into a single geopotential residual at the level where the wind is desired. This is due to the reference level implied in the complete temperature profile and the statistical relationship between height and temperature residuals. In practice, then, if temperature residuals are to be used to calculate geostrophically-related wind residuals, the entire temperature profile must be considered.

Table 2. Experiments with cross-correlation analysis, using temperature and height residuals to determine wind residuals. See text for explanation.

Pressure (mb)	t(°C)	h(m)	All t	All h	Weights h_{400}	t_{450}, t_{350}
85	-1.9		+0.9			-
100		+4.4		0	-	
125	-1.1		+0.14			-
150		+15.8		0	-	
175	-0.2		+0.16			-
200		+17.7		-0.02	-	
225	+0.2		+0.14			-
250		+16.5		+0.05	-	
275	+0.5		+0.17			-
300		+14.0		-0.05	-	
350	+1.0		+0.20			+0.18
400		+5.9		-0.49	-0.53	
450	+1.4		-0.13			-0.19
500		-2.9		-0.03	-	
600	+1.3		-0.15			-
700		-14.3		+0.02	-	
777	-0.1		-0.07			-
850		-13.9		-0.02	-	
928	-0.9		-0.08			-
1000		-9.9		+0.01	-	
	u_{400}		-0.43	-0.43	-0.43	-0.07

Interobservation Correlations

Consider a grid point g with two observations (F_1°, F_2°) nearby to correct the estimate $\hat{F}_g$ at g. In accordance with eqn. (4)

$$F_g^a = \hat{F}_g + a_1(F_1^\circ - \hat{F}_1) + a_2(F_2^\circ - \hat{F}_2). \tag{34}$$

It is recognized that F_1^o are erroneous to some extent: thus

$$F_g^a = \hat{F}_g + a_1(F_1 - \hat{F}_1 + \varepsilon_1) + a_2(F_2 - \hat{F}_2 + \varepsilon_2) \tag{35}$$

where it will be remembered that $F^o = F + \varepsilon$. According to eqn. (8), minimization of the mean-square expected interpolation error yields the following two equations in the unknown coefficients a_1 and a_2:

$$\begin{aligned} (\sigma_1^2 + \varepsilon_1^2)a_1 + (\overline{f_1 f_2} + \overline{\varepsilon_1 \varepsilon_2})a_2 &= \overline{f_g f_1} \\ (\overline{f_2 f_1} + \overline{\varepsilon_2 \varepsilon_1})a_1 + (\sigma_2^2 + \varepsilon_2^2)a_2 &= \overline{f_g f_2}, \end{aligned} \tag{36}$$

where the various correlations between truth and error have been neglected, and $\sigma_1^2 = \overline{f_1 f_1}$. This pair of equations may be solved to obtain

$$a_2 = \frac{\overline{f_g f_2}}{\sigma_2^2+\varepsilon_2^2} - \frac{(\overline{f_1 f_2} + \overline{\varepsilon_1 \varepsilon_2})}{\sigma_2^2 + \varepsilon_2^2}\left(\frac{\overline{f_g f_1}(\sigma_2^2+\varepsilon_2^2) - (\overline{f_1 f_2}+\overline{\varepsilon_1 \varepsilon_2})\overline{f_g f_2}}{(\sigma_1^2+\varepsilon_1^2)(\sigma_2^2+\varepsilon_2^2) - (\overline{f_1 f_2}+\overline{\varepsilon_1 \varepsilon_2})^2}\right) \quad (37)$$

and

$$a_1 = \frac{\overline{f_g f_1}(\sigma_2^2 + \varepsilon_2^2) - (\overline{f_1 f_2} + \overline{\varepsilon_1 \varepsilon_2})\overline{f_g f_2}}{(\sigma_1^2+\varepsilon_1^2)(\sigma_2^2+\varepsilon_2^2) - (\overline{f_1 f_2}+\overline{\varepsilon_1 \varepsilon_2})^2} \quad (38)$$

In order to focus on the effect of interobservational correlation, we assume perfect data: $\varepsilon_1 = \varepsilon_2 = 0$. Then the weights are

$$a_2 = \frac{\overline{f_g f_2}}{\sigma_2^2} - \frac{\overline{f_1 f_2}}{\sigma_2^2}\left(\frac{\overline{f_g f_1}\,\sigma_2^2 - \overline{f_1 f_2}\;\overline{f_g f_2}}{\sigma_1^2\,\sigma_2^2 - (\overline{f_1 f_2})^2}\right) \quad (39)$$

$$a_1 = \frac{\overline{f_g f_1}\,\sigma_2^2 - \overline{f_1 f_2}\;\overline{f_g f_2}}{\sigma_1^2\,\sigma_2^2 - (\overline{f_1 f_2})^2} \quad (40)$$

If the observations are uncorrelated, $\overline{f_2 f_1} = \overline{f_1 f_2} = 0$, and we obtain

$$a_2 = \frac{\overline{f_g f_2}}{\sigma_2^2} \quad (41)$$

$$a_1 = \frac{\overline{f_g f_1}}{\sigma_1^2}\ ; \quad (42)$$

thus the weight assigned each of the two observations is given by the correlation of the observation with the grid point.

The relationahip between the covariance and correlation functions is $\overline{f_1 f_2} = \sigma_1 \sigma_2\, \rho_{12}$, where ρ is the correlation. If the observations are perfectly correlated, then the covariance may be replaced by

$$\overline{f_1 f_2} = \sigma_1 \sigma_2,$$

because the correlation $\rho = 1$. Then it may be seen that the denominators in (39) and (40) vanish. This represents a violation of the linear system, since the equations are no longer independent.

Next consider the case in which the correlation ρ is between zero and unity. Then the weights are given by

$$a_2 = \frac{G_2}{\sigma_2^2} - \frac{G_2}{\sigma_2^2}\rho\sigma_1\sigma_2 \frac{(G_1/G_2)\sigma_2^2 - \rho\sigma_1\sigma_2}{\sigma_1^2\sigma_2^2(1-\rho^2)} \tag{43}$$

and

$$a_1 = \frac{G_1}{\sigma_1^2} \frac{\sigma_2^2 - \sigma_1\sigma_2\,\rho(G_2/G_1)}{\sigma_2^2(1-\rho^2)}$$

where $G_1 \equiv \overline{f_g f_1}$, $G_2 \equiv \overline{f_g f_2}$. Note that G_1/σ_1^2, G_2/σ_2^2 are the weights for the case when the two observations are uncorrelated. We further simplify by assuming that the observations are of the same variable, so that $\sigma_1 = \sigma_2$. We also assume for simplicity that the covariances between observations and grid point depend on distance only, and that the two observations are equidistant from the grid point, so that $\overline{f_g f_1} = \overline{f_g f_2} \equiv G$. Under these circumstances the weights reduce to

$$a_1 = a_2 = \frac{G}{\sigma^2}\left(\frac{1}{1+\rho}\right) \tag{45}$$

For observations which are positively correlated, the weight accorded each is reduced by comparison to data which are not correlated. This is a reflection of less independent information in two observations which are correlated than in two which are not. It is worth noting that the recognition given interobservational correlation is a prime distinguishing feature of the statistical interpolation method by comparison to, for example, a successive-corrections method.

Effect of Random Errors

We now reconsider eqns. (37) and (38), and assume that the two observations are uncorrelated, but have random errors; but $\varepsilon_1, \varepsilon_2 \neq 0$. The weights then become

$$a_2 = G_2/(\sigma_2^2 + \varepsilon_2^2) \tag{46}$$

$$a_1 = G_1/(\sigma_1^2 + \varepsilon_1^2). \tag{47}$$

All else being equal, the effect of random observational error is to reduce the weight given the data. By default (see eqn. 35), this increases the influence of the background field in the final analysis.

Effect of Correlated Errors

We now remove the assumption that $\overline{\varepsilon_1 \varepsilon_2} = 0$. For simplicity, we will continue to assume that the true forecast errors are uncorrelated ($\overline{f_1 f_2} = 0$), but that the observational system exhibits a large-scale bias, so that $\overline{\varepsilon_1 \varepsilon_2} \neq 0$. Then the weights become

$$a_2 = \frac{G_2}{\sigma_2^2 \varepsilon_2^2} - \frac{\overline{\varepsilon_1 \varepsilon_2}}{\sigma_2^2 + \varepsilon_2^2} \frac{G_1(\sigma_2^2 + \varepsilon_2^2) - \overline{\varepsilon_1 \varepsilon_2} G_2}{(\sigma_1^2 + G_1^2)(\sigma_2^2 + \varepsilon_2^2) - (\overline{\varepsilon_1 \varepsilon_2})^2} \tag{48}$$

$$a_1 = \frac{G_1(\sigma_2^2 + \varepsilon_2^2) - \overline{\varepsilon_1 \varepsilon_2} G_2}{(\sigma_1^2 + \varepsilon_1^2)(\sigma_2^2 + \varepsilon_2^2) - (\overline{\varepsilon_1 \varepsilon_2})^2} \tag{49}$$

To further simplify, we assume

$$G_1 = G_2$$

$$\sigma_1^2 = \sigma_2^2$$

$$\varepsilon_1^2 = \varepsilon_2^2.$$

The weights reduce to

$$a_1 = a_2 = \frac{G}{\sigma^2 + \varepsilon^2}\left(1 - \frac{\varepsilon_1 \varepsilon_2}{\sigma^2 + \varepsilon^2 + \overline{\varepsilon_1 \varepsilon_2}}\right) = \frac{G}{\sigma^2 + \varepsilon^2 + \overline{\varepsilon_1 \varepsilon_2}}. \tag{50}$$

Therefore, the effect of correlated observational errors is also to reduce the weight of the observations, beyond the reduction introduced by random errors. It should be noted, however, that this applies only to univariate analysis. Bergman (1978) and Seaman (1977) have shown that correlated errors in mass observations can improve wind analyses.

Extrapolation

Finally, we note a peculiarity of statistical interpolation which has previously been mentioned by Kruger (1969), among others. This problem arises when pairs of observations are close together and are approximately collinear with the grid point being analyzed. Under these circumstances, the datum closest to the grid point has its weight increased, while that furthest away has its weight decreased, even becoming negative. The result is that the analyzed residual may be larger than either of the observed residuals; hence, the term 'extrapolation.' This behavior can be examined by considering two observations located some distance from the grid point being analyzed, as in Fig. 11.

We imagine the positions of the two data points outlining a circle of radius r, the center of which is a distance x from the grid point. The data points will be allowed to move around the circle to encompass several positions, including those indicated in Fig. 11. In any position the data are separated from the grid point by distances R_1 and R_2 and from each other by the circle's diameter 2r.

For simplicity, we assume the data to be error-free. The analysis equation is then

$$F^a = f_g + a_1 F_1^o + a_2 F_2^o, \tag{51}$$

and the weights a_1, a_2 are determined by solving the pair of equations

$$\begin{aligned} \sigma_1^2 a_1 + \overline{f_1 f_2}\, a_2 &= \overline{f_g f_1} \\ \overline{f_2 f_1}\, a_1 + \sigma_2^2 a_2 &= \overline{f_g f_2} \,. \end{aligned} \tag{52}$$

However, it is somewhat more convenient to pursue the argument after normalization by the forecast error variance $\sigma_1^2 = \sigma_2^2 = \sigma^2$:

$$\begin{aligned} a_1 + \rho a_2 &= G_1 \\ \rho a_1 + a_2 &= G_2 \,, \end{aligned} \tag{53}$$

where

$$\overline{f_1 f_2} = \sigma^2 \rho$$

and

$$G_1 = \frac{\overline{f_g f_i}}{\sigma^2} \,.$$

We may then write the solution as

$$a_1 = G_1 - \rho a_2 \tag{54}$$

$$a_2 = \frac{G_2 - \rho G_1}{1 - \rho^2} \,. \tag{55}$$

Now consider the case when the angle θ in Fig. 11 is equal to 90°: if the correlations are assumed to be functions of distance only, then $G_2 = G_1$ since the two data points are equidistant from the grid point. The weights become

$$a_1 = a_2 = \frac{G}{1 + \rho} . \tag{56}$$

That is, the weights are identical, and both are diminished by the inter-observational correlation ρ.

We next consider the two observations approximately collinear with the grid point. Since we have assumed that the correlation function depends on distance only, $G_1 > G_2$. If r is small enough, the inter-observational correlation will be large enough so that $G_2 \leq \rho G_1$. The weight on the observation farthest from the grid point, a_2, is thus zero or negative for the equality or inequality, respectively.

Thus, when $\theta = 90°$, the weights are equal and positive. As θ decreases, an angle is reached where the equality holds. At that point, $a_2 = 0$: the observation receives no weight. For smaller angles, $a_2 < 0$. When this occurs, any gradient in the observed residuals is magnified as it is extrapolated to the grid point.

We may note several points concerning this configuration:

1) The two observations need be only approximately collinear with the grid point;

2) As $\rho \to 1$, a_2 becomes large negative and a_1 becomes large positive. Thus, the closer the two observations are to each other, and the closer they are to collinearity with the grid point, the more exaggerated is the extrapolated solution;

3) As $G_1 \to 1$, the larger must be the interobservational correlation in order to force $a_2 < 0$. Thus, as the first observation is located closer to the grid point, the less likely it is that an exaggerated extrapolation will occur.

4) The problem can be avoided by not considering highly-correlated observations in the analysis; observations which are located close together probably should be averaged into one datum prior to the analysis.

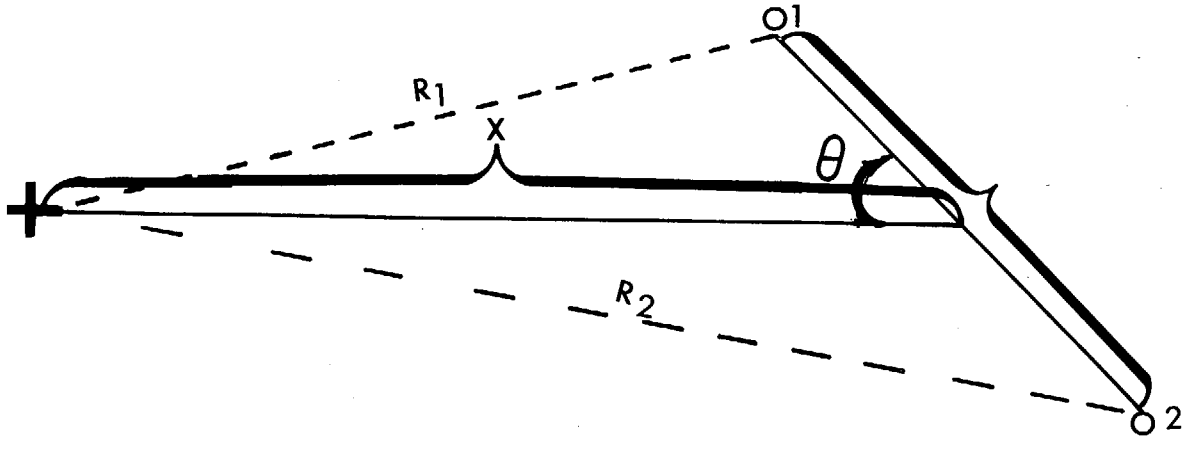

Figure 11. Schematic example of arrangement of data (circles) which can lead to an extrapolation solution to the grid point (cross).

V. Summary

The theory of statistical interpolation has been described in general terms. Attractive aspects of the method, such as its ability to account for data distribution through the interobservational correlation, and its accounting for random and correlated observation errors, have been examined and illustrated. It is worth repeating that this theory rests on a number of assumptions:

- the forecast error statistics are at least locally homogeneous;
- the mean forecast error is zero;
- three-dimensional correlation functions can be represented as a product of horizontal and vertical components;
- analytic functions are sufficient to model the actual correlation functions;
- analyzed corrections to the mass and motion fields are related hydrostatically and geostrophically.

Additional assumptions are necessary for practical application, and these are discussed in the next lecture of this series.

APPENDIX

The $\rho(ht)$ cross-correlation may be determined from the appropriate entry in the covariance table (Table 1) and eqn. (11):

$$\sigma_h\sigma_t\ \rho(ht) = \overline{ht} = -\frac{g}{R}\frac{\partial}{\partial q}(\overline{hh}) = \frac{g}{R}\frac{\partial}{\partial q}\left\{\sigma^2[1 + K_p q^2]^{-1}\right\}$$

where $q = \ln P_i/P_j$, i being associated with h_{250}, and j being associated with the various t values. Note that we have assumed no horizontal separation between points i and j, so that the horizontal covariance component is unity. Performing the indicated differentiation, we obtain

$$\rho(ht) = \left(\frac{2K_p g}{R}\right) q \frac{\sigma_h}{\sigma_t}(\overline{hh})^2$$

assuming that σ_h^2 is invariant with q. By a similar procedure, we may develop the following expression for $\rho(ut)$:

$$\rho(ut) = \frac{g^2}{fR}\left(\frac{\sigma_h}{\sigma_u}\right)\left(\frac{\sigma_h}{\sigma_t}\right)\left(-2K_h e^{\frac{1}{2}}\right)\left(2K_p q\right)(\overline{hh})^2$$

where we have assumed that $\frac{\partial}{\partial y}[e^{-K_h s^2}]$ = maximum as well as that σ_h^2 is constant. In order to determine the ratios σ_h/σ_u and σ_h/σ_t, we note that from Table 1 that

$$\overline{u(\eta)\ u(y)} = \frac{g^2}{f^2}\frac{\partial^2}{\partial\eta\ \partial y}\overline{hh},$$

and with eqn. (11)

$$\overline{u(\eta)\ u(y)} = \sigma_h^2\ \frac{g^2}{f^2}\ (2K_h)[1 - 2K_h(\eta-y)^2]\ e^{-K_h(\eta-y)^2}$$

where the vertical component is assumed to be unity. At zero separation ($\eta = y$), the left side becomes σ_u^2, and we have

$$\sigma_u^2 = \sigma_h^2\ \frac{g^2}{g^2}(2K_h),$$

or

$$\sigma_h/\sigma_u = \frac{f}{g\sqrt{2K_h}}\ .$$

Similarly, from Table 1

$$\overline{t(\zeta)\ t(z)} = \left(\frac{g}{R}\right)^2\ \frac{\partial^2}{\partial\zeta\partial z}(\overline{hh})$$

and from eqn. (11), with zero horizontal separation,

$$\overline{t(\zeta)\ t(z)} = -\ 2K_p\left(\frac{g^2}{R^2}\right)^2 \sigma_h^2\,[1 + K_p(\zeta-z)^2]^{-2}\cdot$$

$$\left(1 - 4K_p(\zeta-z)^2[1 + K_p(\zeta-z)^2]^{-1}\right).$$

As the separation $(\zeta-z)$ vanishes, the left side becomes σ_t^2, and we have

$$\sigma_t^2 = 2K_p\left(\frac{g^2}{R^2}\right)\sigma_h^2,$$

or

$$\sigma_h/\sigma_t = \frac{R}{g\sqrt{2K_p}}\ .$$

Therefore, for $\sigma_h^2 = 40\ m^2$ we can determine the ratios as

$$\sigma_h/\sigma_t = 9.26\ m\ deg^{-1},$$

and

$$\sigma_h/\sigma_u = 5.26 \times 10^{-3} m(m\ sec^{-1})^{-1}\ .$$

It is worth noting in passing that independent knowledge of σ_h, σ_t, and σ_u is sufficient to determine K_h and K_p.

References

Bergman, K., 1978: The role of observational errors in optimum interpolation analysis. Bull. Amer. Meteor. Soc., 59, 1604-1611.

_____, 1979: Multivariate analysis of temperatures and winds using optimum interpolation. Mon. Wea. Rev., 107, 1423-1444.

Gandin, L., 1963: Objective analysis of meteorological fields. Gidrometeorologichoskoe Isdatel'stvo, Leningrad. Translated from Russian, Israel Program for Scientific Translation, Jerusalem, 1965, 242 pp.

Kruger, H., 1969: General and special approaches to the problem of objective analysis of meteorological fields. Quart. J. Roy. Meteor. Soc., 95, 21-39.

Lorenc, A., I. Rutherford, and G. Larsen, 1977: The ECMWF analysis and data assimilation scheme--analysis of mass and wind fields, European Centre for Medium Range Weather Forecasts, Tech. Rpt. 6.

McPherson, R., K. Bergman, R. Kistler, G. Rasch, and D. Gordon, 1979: The NMC global data assimilation system. Mon. Wea. Rev., 107, 1445-1461.

Miyakoda, K., R. Strickler, and J. Chlodzinski, 1978: Initialization with with the data assimilation method. Tellus, 30, 32-54.

Rutherford, I., 1972: Data assimilation by statistical interpolation of forecast error fields. J. Atmos. Sci., 29, 809-815.

Schlatter, T., 1975: Some experiments with a multivariate statistical objective analysis scheme. Mon. Wea. Rev., 103, 246-257.

Seaman, R., 1977: Absolute and differential accuracy of analyses achievable with specified observational network characteristics. Mon. Wea. Rev., 105, 1211-1222.

Thiebaux, H., 1975: Experiments with correlation representations for objective analysis. Mon. Wea. Rev., 103, 617-627.